RNA ligase RtcB splices 3′-phosphate and 5′-OH ends via covalent RtcB-(histidinyl)-GMP and polynucleotide-(3′)pp(5′)G intermediates

Anupam K. Chakravarty[a], Roman Subbotin[b], Brian T. Chait[b], and Stewart Shuman[a,1]

[a]Molecular Biology Program, Sloan-Kettering Institute, New York, NY 10065; and [b]Laboratory for Mass Spectrometry and Gaseous Ion Chemistry, Rockefeller University, New York, NY 10065

Edited by Olke C. Uhlenbeck, Northwestern University, Evanston, IL, and approved February 28, 2012 (received for review January 21, 2012)

A cherished tenet of nucleic acid enzymology holds that synthesis of polynucleotide 3′-5′ phosphodiesters proceeds via the attack of a 3′-OH on a high-energy 5′ phosphoanhydride: either a nucleoside 5′-triphosphate in the case of RNA/DNA polymerases or an adenylylated intermediate A(5′)pp(5′)N– in the case of polynucleotide ligases. RtcB exemplifies a family of RNA ligases implicated in tRNA splicing and repair. Unlike classic ligases, RtcB seals broken RNAs with 3′-phosphate and 5′-OH ends. Here we show that RtcB executes a three-step ligation pathway entailing (*i*) reaction of His337 of the enzyme with GTP to form a covalent RtcB-(histidinyl-N)-GMP intermediate; (*ii*) transfer of guanylate to a polynucleotide 3′-phosphate to form a polynucleotide-(3′)pp(5′)G intermediate; and (*iii*) attack of a 5′-OH on the –N(3′)pp(5′)G end to form the splice junction. RtcB is structurally *sui generis*, and its chemical mechanism is unique. The wide distribution of RtcB proteins in bacteria, archaea, and metazoa raises the prospect of an alternative enzymology based on covalently activated 3′ ends.

covalent catalysis | RNA repair

ATP-dependent RNA and DNA ligases join broken 3′-OH and 5′-PO_4 polynucleotide ends via three nucleotidyl transfer steps: (*i*) ligase reacts with ATP to form a ligase-(lysyl-N)–AMP intermediate plus pyrophosphate; (*ii*) AMP is transferred from ligase-adenylate to the 5′-monophosphate RNA end to form a polynucleotide-adenylate intermediate, A(5′)pp(5′)RNA or A(5′)pp(5′)DNA; and (*iii*) ligase catalyzes attack by a polynucleotide 3′-OH on A(5′)pp(5′)RNA/DNA to form a 3′-5′ phosphodiester bond and release AMP (1). The salient principle of classic ligase catalysis is that the high energy of the ATP phosphoanhydride bond is transferred via the enzyme to the polynucleotide 5′ end, thereby activating the 5′ end for phosphodiester synthesis, with AMP as a favorable leaving group. The shared chemical mechanism of classic RNA and DNA ligases is reflected in their conserved core tertiary structures and active sites (1).

Classic ATP-dependent RNA ligases are encoded by diverse taxa in all three phylogenetic domains. In bacteria, fungi, and plants they function as components of multienzyme RNA repair pathways that heal and seal broken RNAs with 2′,3′ cyclic phosphate and 5′-OH ends (2–5). In the healing phase, the 2′,3′ cyclic phosphate end is hydrolyzed by a phosphoesterase enzyme to a 3′-OH, and the 5′-OH end is phosphorylated by a polynucleotide kinase enzyme to yield a 5′-monophosphate. The resulting 3′-OH and 5′-phosphate ends are then suitable for ATP-dependent sealing by RNA ligase. This "healing-and-sealing" pathway is responsible for tRNA splicing in fungi and plants (6, 7), for mRNA splicing in the fungal unfolded protein response (8), and for tRNA restriction repair during bacteriophage infection of *Escherichia coli* (9).

An alternative "direct ligation" pathway for joining 2′,3′ cyclic phosphate and 5′-OH ends during mammalian tRNA splicing was discovered nearly 30 y ago (10–12), when it was shown that the 2′,3′ cyclic phosphate of the cleaved pre-tRNA is incorporated at the splice junction in the mature tRNA. (The junction phosphate in yeast tRNA splicing derives from the γ-phosphate of the NTP substrate for the 5′ kinase step.) Direct ligation languished until 2011, when three laboratories identified bacterial, archaeal, and mammalian RtcB proteins as RNA ligase enzymes capable of sealing 2′,3′ cyclic phosphate and 5′-OH ends (13–15). In support of a bona fide RNA repair function for RtcB in vivo, it was shown that *E. coli* RtcB is competent and sufficient for eukaryal tRNA splicing, by virtue of its ability to complement growth of yeast cells that lack the endogenous healing-and-sealing-type tRNA ligation system (16). Moreover, RtcB can replace yeast tRNA ligase as the catalyst of *HAC1* mRNA splicing during the unfolded protein response (16).

RtcB is unique with respect to its tertiary structure and the architecture of its active site (16, 17), hinting at an unprecedented mechanism of end-joining. Parsimony and energetics suggested a one-step mechanism for sealing via attack by the O5′ nucleophile on the cyclic phosphate, with expulsion of the ribose O2′ and generation of a 3′,5′ phosphodiester at the splice junction. However, we found that RtcB violates Occam's razor, insofar as it executes a two-step pathway of strand joining whereby the 2′,3′ cyclic phosphodiester end is hydrolyzed to a 3′-monophosphate, which is then ligated to the 5′-OH end to form the splice junction (18).

A remarkable finding was that the 3′-phosphate ligase activity of RtcB requires GTP or dGTP (18). Neither ATP nor any other nonguanosine NTP sustains RtcB's ligase activity. The finding that GTP reacts with RtcB to form a covalent RtcB–guanylate adduct (18) raised the prospect that GTP might provide the chemical energy for a polynucleotide ligation reaction. Here we characterize the nature of the covalent RtcB–GMP adduct, establish its essentiality for end-joining, and identify polynucleotide-(3′)pp(5′)G as a second covalent intermediate in a three-step pathway for sealing 3′-phosphate/5′-OH breaks.

Results and Discussion

GTP-Dependent RNA End-Joining. The requirement for GTP is illustrated in Fig. 1, where the substrate for ligation is a 20-mer RNA strand with 5′-OH and 3′-monophosphate ends and a single radiolabel between the 3′-terminal and penultimate nucleosides. Reaction of $_{HO}$RNAp with RtcB and GTP yielded a more rapidly migrating circular RNA species as a consequence of intramolecular sealing. No ligation was detected in the absence of added GTP. Ligation increased with GTP concentration in the range of 0.1–1 μM and was complete at 6.25 μM GTP. The observation that 65% of the substrate was ligated at 1 μM GTP (when GTP was in just 10-fold excess over input RNA) attests to the efficiency of GTP utilization.

Author contributions: A.K.C., R.S., and S.S. designed research; A.K.C. and R.S. performed research; A.K.C., R.S., B.T.C., and S.S. analyzed data; and A.K.C. and S.S. wrote the paper.

The authors declare no conflict of interest.

This article is a PNAS Direct Submission.

[1]To whom correspondence should be addressed. E-mail: s-shuman@ski.mskcc.org.

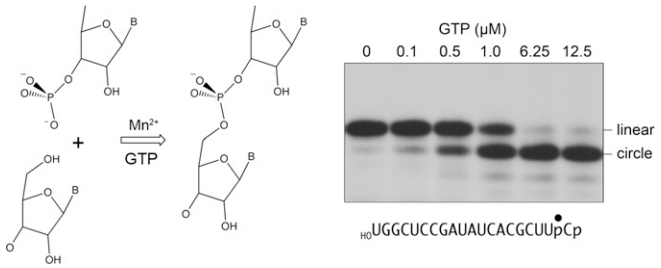

Fig. 1. RtcB is a GTP-dependent 3′-phosphate/5′-OH RNA ligase. RtcB splices a 3′-monophosphate RNA end to a 5′-OH end in a reaction that requires manganese and GTP. The dependence of ligation on GTP concentration is shown. Reaction mixtures containing 2 mM $MnCl_2$, 0.1 μM 20-mer RNA (depicted at bottom with the ^{32}P-label denoted by ●), 1 μM RtcB, and GTP as specified were incubated at 37 °C for 30 min. The labeled RNAs were resolved by PAGE. Intramolecular end-joining by RtcB converts the linear substrate to more rapidly migrating circular product.

Histidine-337 Is the Site of Covalent Guanylylation. The RtcB–[^{32}P] guanylate adduct formed by reaction of *E. coli* RtcB with [α^{32}P] GTP was sensitive to acid and hydroxylamine but resistant to alkali, consistent with a P–N bond (18). To map the site of covalent guanylylation within the 408-aa RtcB polypeptide, we reacted the recombinant protein in vitro with unlabeled GTP, then subjected the sample to cysteine reduction and alkylation with iodoacetamide, followed by proteolysis with trypsin. The tryptic peptides were analyzed by HPLC interfaced with nano-electrospray ionization mass spectrometry (19). We thereby identified a species with a *m/z* value of 723.93, consistent with a GMP adduct of the tryptic peptide ^{325}GLGNEESFCSCSHGAGR^{341} (measured molecular mass 2,168.777; calculated molecular mass 2,168.778) in which both cysteines were alkylated and the net charge is +3 (Fig. 2*A* and *B*). The guanylylated species, eluting at 22.38 min during HPLC, was resolved from the unguanylylated version of the same tryptic peptide, which eluted at 21.34 min (Fig. 2*A*). Within this tryptic peptide, His337 is the only plausible site of GMP attachment via a P–N bond.

Further analysis of the guanylylated tryptic peptide by tandem mass spectrometry is shown in Fig. 3. Fragmentation of the GMP–peptide adduct yielded the unguanylylated intact peptide (species denoted as $[-GMP]^{2+}$ in Fig. 3*B*, with *m/z* of 903.9) and GMP as major products, consistent with the fragility of the P–N bond under the acidic conditions used (Fig. 3*A*). Additional *m/z* signatures were observed for a phosphopeptide arising by subtraction of guanosine during fragmentation (species denoted as $[-Guan]^{2+}$, with *m/z* of 951.9) and for phosphoribosyl–peptide adducts reflective of scission of the glycoside bond with loss of guanine (Fig. 3 *A* and *B*). Two minor fragmentation products, corresponding to peptides b13 (^{325}GLGNEESFCSCSH^{337}) and y11 (^{331}SFCSCSHGAGR^{341}) were also detected (Fig. 3 *B* and *C*), providing affirmation of the assignment of the sequence of the parent tryptic peptide.

His337 is conserved in all RtcB homologs and is essential for *E. coli* RtcB's tRNA splicing activity in vivo (16). His337 is situated in the RtcB active site immediately adjacent to a cluster of putative metal-binding side chains (17). To probe the role of His337 in RtcB guanylylation, we purified missense mutants of *E. coli* RtcB in which His337 was either replaced by alanine or substituted conservatively with asparagine or glutamine (Fig. 4*A*). Whereas wild-type RtcB reacted with 10 μM [α^{32}P]GTP to form an SDS-resistant 45-kDa RtcB–[^{32}P]GMP adduct, the H337A, H337N, and H337Q proteins were inert (Fig. 4*B*). Moreover, the H337A, H337N and H337Q mutations abolished 3′-phosphate/5′-OH RNA ligation (Fig. 4*C*). These results support the assignment of His337 as the nucleophile in the RtcB guanylylation reaction and the intermediacy of RtcB–GMP in RNA end-joining.

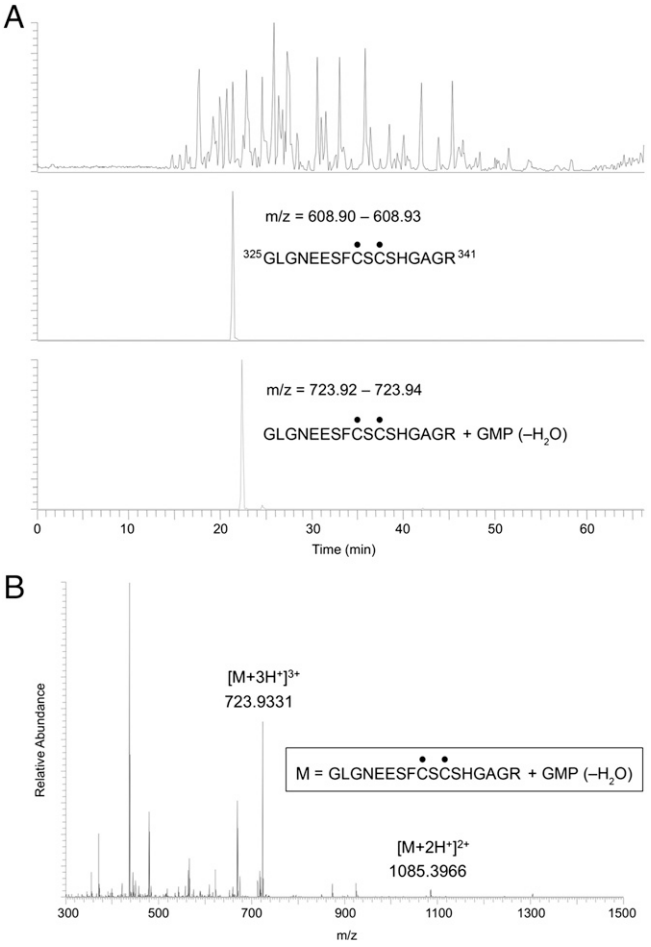

Fig. 2. Identification of a guanylylated RtcB tryptic peptide. (*A*) *Top*: Mass chromatogram of the mixture of tryptic peptides derived from RtcB after in vitro reaction with cold GTP. *Bottom*: Elution profile of a peptide with *m/z* of 732.92–732.94, consistent with a GMP adduct of the tryptic peptide ^{325}GLGNEESFCSCSHGAGR^{341} in which both cysteines were alkylated (denoted by ● over the C residues) and the net charge is +3. *Middle*: Elution profile of a peptide with *m/z* of 608.90–608.93, corresponding to the unguanylylated version of the same tryptic peptide, in which both cysteines were alkylated and the net charge is +3. (*B*) Mass spectrum of the guanylylated peptide M. The peaks corresponding to *m/z* values for the peptide designated M with net charges of +3 and +2 are indicated.

RtcB Transfers GMP to a Polynucleotide 3′-Monophosphate End. Experience with classic DNA ligases teaches that the A(5′)pp(5′) DNA intermediate can be difficult to detect under optimal ligation reaction conditions, because the rate of the phosphodiester synthesis step is much faster than the rate of A(5′)pp(5′) DNA formation (20). However, the abundance and persistence of the adenylylated polynucleotide in the classic ligase scheme can be enhanced by nucleic acid modifications that slow the final step (21). With this in mind, we sought to demonstrate transfer of [^{32}P]GMP to the 3′-monophosphate terminus of a DNA polynucleotide, reasoning that an all-DNA strand might be ineffective, or at least less effective than RNA, as a substrate for the full ligation reaction. Fig. 5*A* shows that RtcB does indeed transfer [^{32}P]guanylate from GTP to an unlabeled 3′-phosphate-terminated 23-mer DNA. The yield of the labeled polynucleotide increased with the amount of input 3′-phosphate polynucleotide (Fig. 5*A*). The polynucleotide guanylylation reaction reached an endpoint at 5–15 min with ≈25% of the input cold 23-mer becoming ^{32}P-labeled; the reaction attained half of the endpoint value in <1 min (Fig. 5*B*). Note that there was no detectable

BIOCHEMISTRY

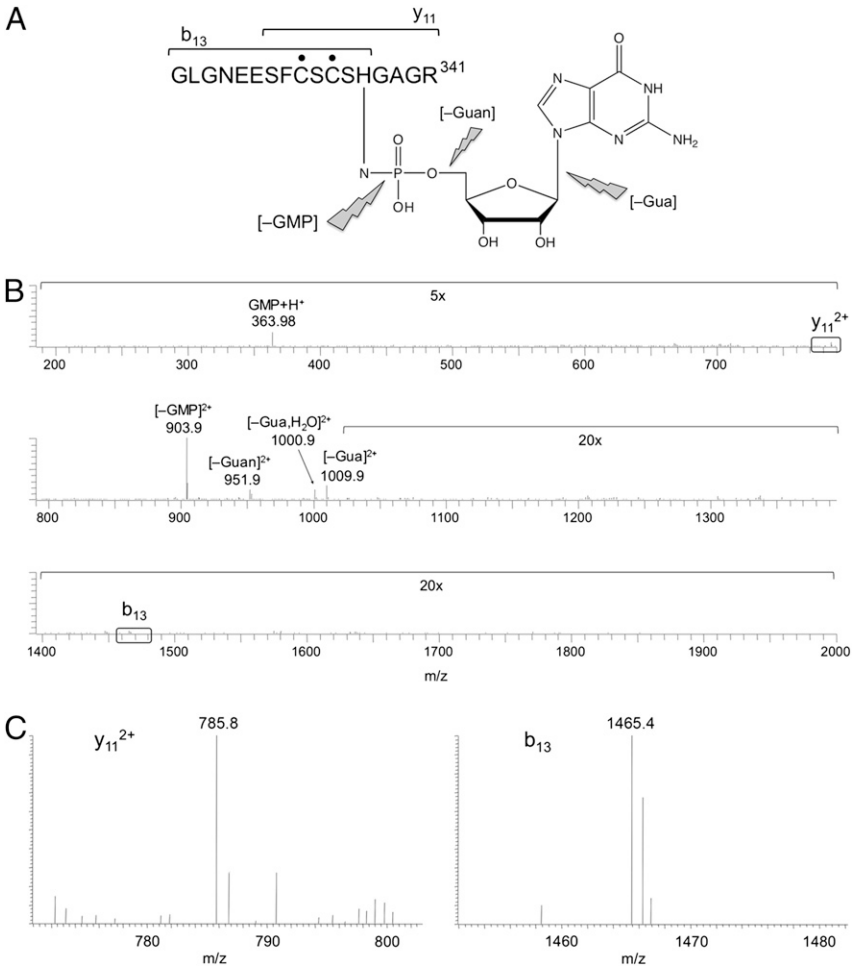

Fig. 3. Identification of His337 as the site of guanylylation. (*A*) Depiction of the His337-guanylylated tryptic peptide. The sites of fragmentation of the guanylate moiety during tandem mass spectrometry are shown. Two unguanylylated peptide fragments, y11 and b13, detected in the MS/MS analysis are demarcated by brackets. (*B*) Nano-electrospray ionization MS/MS analysis of the guanylylated RtcB tryptic peptide. The unamplified peaks corresponding to the 17-aa peptides with +2 net charge after loss of GMP, guanosine (Guan), or guanine (Gua; alone or with water) are indicated. The 5× amplified region of the spectrum that includes GMP and peptide fragment $y11^{2+}$ and the 20× amplified portion of the spectrum that includes peptide fragment b13 are demarcated by brackets. (*C*) Amplified spectra corresponding to peptide fragments $y11^{2+}$ and b13.

label transfer to an otherwise identical 23-mer DNA with a 3′-OH terminus (Fig. 5*A*).

The ^{32}P-labeled 23-mer was gel-purified and analyzed by PEI-cellulose TLC (Fig. 5*C*). All of the label remained at the origin, verifying that there was no residual mononucleotide present. Whereas no radiolabel was released from the DNA by treatment with calf intestine alkaline phosphatase (CIP), nucleotidyl pyrophosphatase (NPP) treatment resulted in quantitative release of the label as [^{32}P]GMP (Fig. 5*C*). Digestion of the labeled DNA with NPP plus CIP released $^{32}P_i$ (Fig. 5*C*). Treatment of the labeled polynucleotide with nuclease P1 (P1), which hydrolyzes 3′O–P bonds, resulted in quantitative release of the label, predominantly as [^{32}P]GDP, with a minority of the P1 product being [^{32}P]GMP (Fig. 5*C*). Dual digestion of the labeled DNA with P1 plus CIP released $^{32}P_i$. This analysis identifies the label-transfer product as polynucleotide-(3′)pp(5′)G.

Polynucleotide-(3′)pp(5′)G Is an Intermediate in the Ligation Reaction. RtcB was reacted in 10-fold enzyme excess with a ^{32}P-labeled 5′-OH/3′-phosphate-terminated 20-mer substrate composed of 19 ribonucleotides and a single 3′-terminal deoxynucleoside. A predominant radiolabeled species migrating ≈2 nucleotide steps above the input 20-mer substrate accumulated at early times (0.5–2 min) and then declined thereafter, concomitant with the progressive formation of the ligated circular RNA product, which migrated ≈2 nucleotide steps below the input 20-mer substrate (Fig. 6*A*). We surmise that the slower-migrating species corresponds to $_{HO}RNA_{19}dC(3')pp(5')G$. The kinetic profiles of the abundance of the $_{HO}RNA_{19}dC(3')pp(5')G$ and ligated species are consistent with a precursor-product relationship (Fig. 6*A*). Fitting the data to a simple two-step kinetic scheme yielded apparent rate constants of 0.87 min^{-1} for the formation of $_{HO}RNA_{19}dC(3')pp(5')G$ and 0.74 min^{-1} for the subsequent step of phosphodiester synthesis.

We conducted a similar kinetic analysis of the reaction of excess RtcB with an all-RNA ^{32}P-labeled 5′-OH/3′-monophosphate-terminated 20-mer. Unlike the 3′-deoxy substrate, in which the $_{HO}RNA_{19}dC(3')pp(5')G$ intermediate constituted 35% of the total labeled material at early times, only trace levels of $_{HO}RNA(3')pp(5')G$ were detectable at 15 and 30 s, constituting ≤1% of the total labeled RNA. The kinetic profile of the ligation of the all-RNA substrate is shown in Fig. 6*B* and is notable for the absence of a lag in the accumulation of the ligated end-products. These results signify that the rate of phosphodiester synthesis during ligation of an all-RNA 3′-phosphate end is much faster (on the order of 50-fold) than the preceding rate of guanylyla-

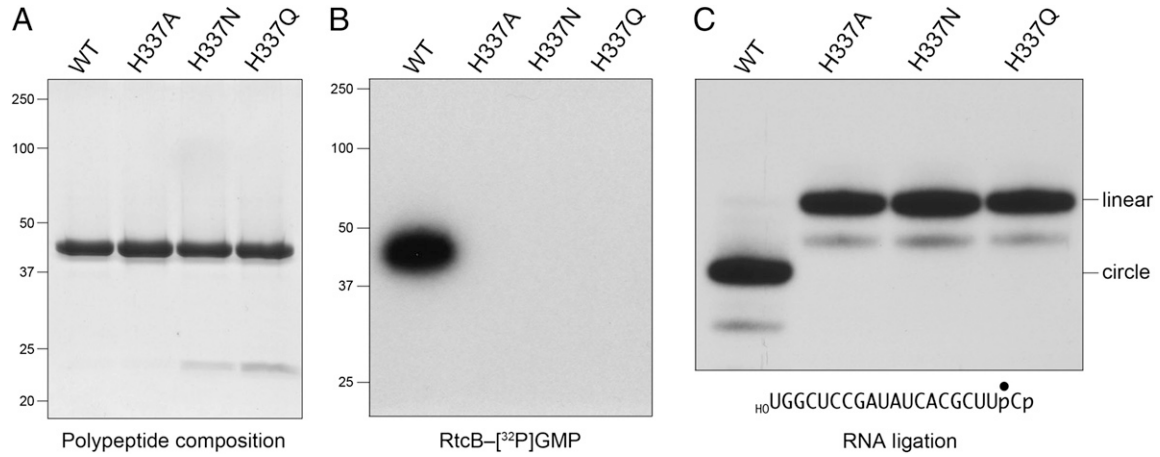

Fig. 4. His337 mutations abolish RtcB guanylylation and RNA ligation. (*A*) Aliquots (5 μg) of the wild-type and mutant RtcB preparations were analyzed by SDS/PAGE. The Coomassie blue-stained gel is shown. The positions and sizes (kDa) of marker proteins are shown at left. (*B*) Label transfer from [α^{32}P]GTP to the wild-type and mutant RtcB proteins was analyzed by SDS/PAGE and autoradiography. (*C*) RNA ligase reaction mixtures containing 2 mM $MnCl_2$, 0.1 μM 20-mer RNA (depicted at bottom with the ^{32}P-labeled denoted by ●), 100 μM GTP, and 1 μM wild-type or mutant RtcB were incubated at 37 °C for 15 min. The labeled RNAs were analyzed by Urea-PAGE.

tion of the 3′-phosphate. Fitting the data in Fig. 6*B* yielded an apparent rate constant of 2.2 min^{-1} for the rate-limiting RNA 3′-guanylylation step; that this value is only 2.5-fold faster than the rate of guanylylation of the 3′-deoxy-terminated substrate (Fig. 6*A*) attests that the terminal ribose 2′-OH is not a major factor in 3′ end activation under the condition tested (i.e., in 100 μM GTP at 10-fold RtcB excess over the nucleic acid substrate). By contrast, the 2′-OH clearly does exert a significant acceleration of phosphodiester synthesis, be it via direct participation in the reaction chemistry or indirectly (e.g., by influencing the conformation of the terminal pentose sugar).

RtcB Executes a Three-Step Pathway of GTP-Dependent RNA Sealing. Here we show how RtcB uses the energy of the α–β phosphoanhydride bond of GTP to splice a 3′-monophosphate end to a 5′-OH end. There are three discrete steps in the RtcB pathway: (*i*) reaction of His337 of the enzyme with GTP to form a covalent RtcB-(histidinyl-N)-GMP intermediate; (*ii*) transfer of guanylate to a polynucleotide 3′-phosphate to form a polynucleotide-(3′)pp(5′)G intermediate; and (*iii*) attack of a 5′-OH on the –N(3′)pp(5′)G end to form the splice junction. To our knowledge there is no antecedent example of enzymatic synthesis of a nucleic acid 3′-5′ phosphodiester via covalent activation of a 3′-monophosphate end to a phosphoanhydride. The accepted "rule" of nucleic acid enzymology is that DNA/RNA polymerases and DNA/RNA ligases generate 3′-5′ phosphodiesters by catalyzing the attack of a primer-strand 3′-OH on the 5′-phosphate of an activated 5′-phosphanhydride: either a nucleoside-5′-triphosphate (polymerases) or an adenylylated A(5′)pp(5′)N– end (ligases). Even the noncanonical "reverse polymerase" activity of the tRNA modification enzyme Thg1 entails the attack of an NTP 3′-OH on the 5′-phosphate of a primer polynucleotide with an activated 5′-phosphanhydride terminus: either an A(5′)pp(5′)N– end or a 5′-triphosphate end (22).

The tertiary structure and active site of RtcB have no similarity whatsoever to those of enzymes known to catalyze covalent nucleotidyl transfer to nucleic acid ends [i.e., classic RNA/DNA ligases (AMP transfer via a lysine-AMP intermediate), mRNA

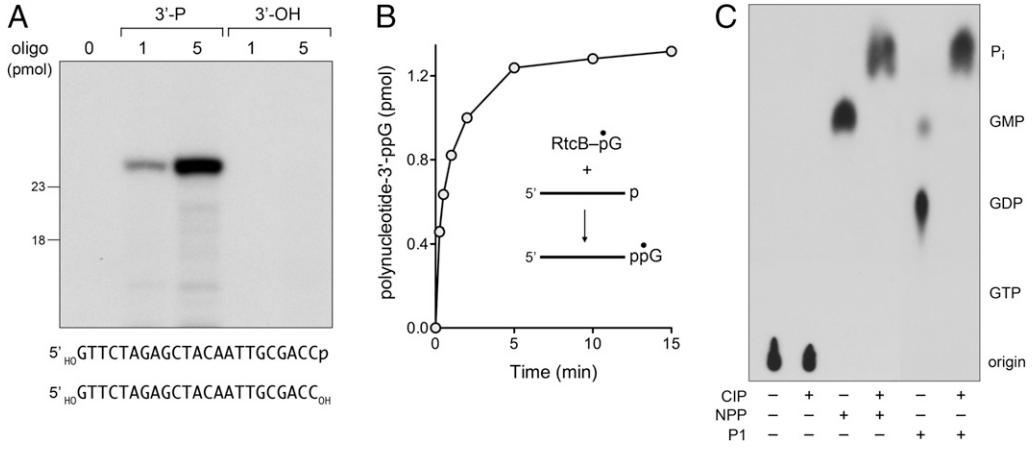

Fig. 5. RtcB transfers GMP to a polynucleotide 3′-monophosphate end. (*A*) Reaction mixtures containing 2 mM $MnCl_2$, 10 μM [α^{32}P]GTP, 5 μM (50 pmol) RtcB, and 0, 1, or 5 pmol of an unlabeled 23-mer DNA with either a 3′-phosphate (3′-P) or a 3′-OH end were incubated for 30 min. The products were analyzed by Urea-PAGE and autoradiography. The 3′-P and 3′-OH DNAs are shown at bottom. (*B*) Kinetics of label transfer to the 3′-phosphate 23-mer DNA (5 pmol input DNA per aliquots analyzed). (*C*) The GMP-labeled 3′-phosphate 23-mer DNA was gel-purified and analyzed by PEI cellulose TLC, without further treatment, or after digestion with alkaline phosphatase (CIP), NPP, or P1, as indicated by +. The positions of cold GTP, GDP, and GMP markers are shown at right.

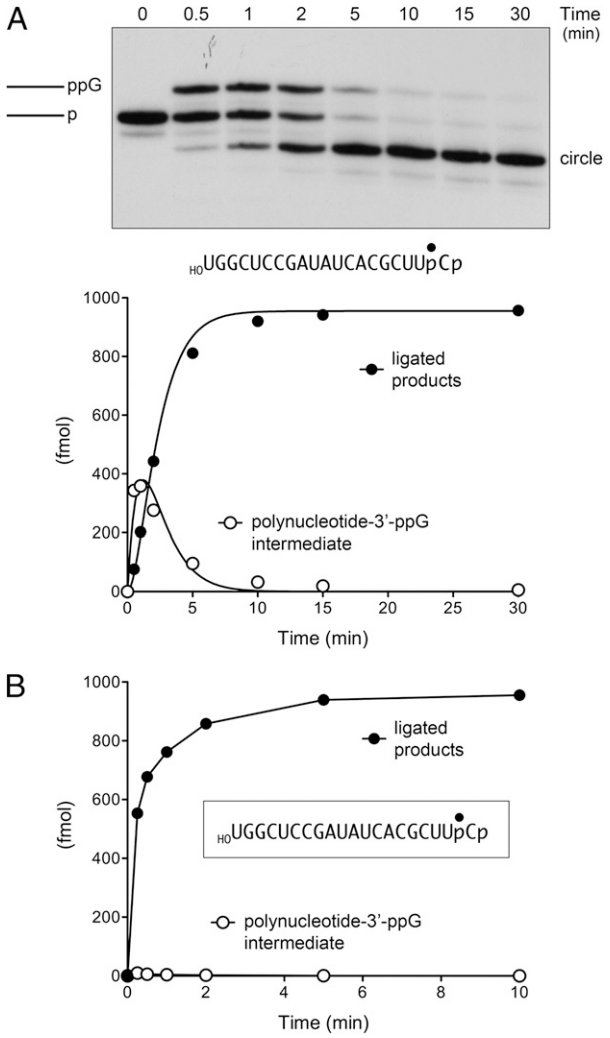

Fig. 6. Polynucleotide-(3′)pp(5′)G is an intermediate in the ligation reaction. (*A*) A reaction mixture (90 μL) containing 2 mM $MnCl_2$, 100 μM GTP, 1 μM RtcB, and 0.1 μM $_{HO}RNA_{19}$(dC)p (depicted with the 3′ deoxynucleoside shaded and the ^{32}P-label denoted by ●) was incubated at 37 °C. Aliquots (10 μL) containing 1 pmol of labeled $_{HO}RNA_{19}$(dC)p substrate were withdrawn at the times specified and quenched immediately. The time 0 sample was withdrawn before adding the enzyme. *Upper*: Products were analyzed by urea-PAGE and visualized by autoradiography. The positions of the linear substrate and guanylylated intermediate are indicated on the left; the position of the ligated circle is indicated on the right. *Lower*: Kinetic profile of the reaction is plotted. A nonlinear regression curve fit of the data (in Prism) to a unidirectional two-step pathway is shown. (*B*) Kinetics of sealing of an all-RNA substrate (depicted with the ^{32}P-labeled denoted by ●) were assayed as described in *A*.

capping enzymes (GMP transfer via a lysine-GMP intermediate), and RNA cyclase (AMP transfer via a histidine-AMP intermediate)] (1, 23). RNA cyclase can covalently adenylate either a polynucleotide 3′-monophosphate end (en route to synthesis of a 2′,3′ cyclic phosphate) or a polynucleotide 5′-monophosphate end (24, 25). However, RNA cyclase is incapable of ligating the activated ends to form a 3′-5′ phosphodiester.

The distinctive mechanism, specificity, and structure of RtcB and the wide distribution of RtcB proteins in bacteria, archaea, and metazoa raise the prospect, indeed the likelihood, that there are other unrecognized catalysts of RNA and DNA synthesis and repair that exploit, or contribute to, a noncanonical enzymology based on activated 3′ ends.

Methods

RtcB Purification. Wild-type *E. coli* RtcB and mutants H337A, H337N, and H337Q were purified to homogeneity as described previously (18). Protein concentrations were determined using the BioRad dye reagent with BSA as the standard.

Ligase Assay. 3′-Phosphorylated 20-mer oligonucleotides labeled with ^{32}P were prepared by enzymatic addition of [5′-^{32}P]**p**Cp or [5′-^{32}P]**p**(dC)p to a 19-mer synthetic oligoribonucleotide and then gel-purified (18). Ligase reaction mixtures (10 μL) containing 50 mM Tris·HCl (pH 8.0), 2 mM $MnCl_2$, GTP as specified, 0.1 μM 5′-$_{HO}$UGGCUCCGAUAUCACGCUU**p**Cp or 5′-$_{HO}$UGGCUCCGAUAUCACGCUU**p**(dC)p, and 1 μM RtcB were incubated at 37 °C. The reactions were quenched by adding 10 μL of 90% (vol/vol) formamide and 50 mM EDTA and then analyzed by electrophoresis through a 40-cm 20% polyacrylamide gel containing 7.5 M urea in 90 mM Tris·borate, 2 mM EDTA. The ^{32}P-labeled RNAs were visualized by autoradiography of the gel and, where specified, quantified by scanning the gel with a Fuji Film BAS-2500 imager.

RtcB Guanylylation Assay. Reaction mixtures (10 μL) containing 50 mM Tris·HCl (pH 8.0), 2 mM $MnCl_2$, 10 μM [α-^{32}P]GTP, and 5 μM wild-type RtcB or mutants H337A, H337N, or H337Q were incubated at 37 °C for 1 min. The reaction was quenched by adding 10 μL of 100 mM Tris·HCl (pH 6.8), 200 mM DTT, 4% (wt/vol) SDS, 20% (vol/vol) glycerol, 0.2% (wt/vol) bromophenol blue, and 10 mM EDTA. The samples were analyzed by SDS/PAGE. Label transfer to the RtcB polypeptide was visualized by autoradiography of the dried gel.

RtcB-Mediated ^{32}P-GMP Transfer from [α^{32}P]GTP to a Polynucleotide-3′-Phosphate. Reaction mixtures (10 μL) containing 50 mM Tris·HCl (pH 8.0), 2 mM $MnCl_2$, 10 μM [α-^{32}P]GTP, and 5 μM RtcB were preincubated for 1 min at 37 °C, then supplemented with 1 pmol or 5 pmol of unlabeled 23-mer DNAs $_{HO}$GTTCTAGAGCTACAATTGCGACCp or $_{HO}$GTTCTAGAGCTACAATTGCGACC$_{OH}$ and incubated for 30 min at 37 °C. The reactions were quenched with formamide and EDTA, and the products were analyzed by urea–PAGE and visualized by autoradiography. To characterize the [^{32}P]GMP linkage to the 3′-phosphate-terminated DNA, the labeling reaction was scaled up to 90 μL and was initiated by adding 45 pmol of unlabeled 23-mer DNA. The labeled polynucleotide was gel-purified and concentrated by ethanol precipitation. Aliquots (200 fmol) of the purified labeled DNA were then treated with CIP, NPP, or P1, singly or in tandem as specified. The CIP reaction mixture (10 μL) containing 50 mM Tris·HCl (pH 7.9), 10 mM $MgCl_2$, 100 mM NaCl, 1 mM DTT, and 1 U CIP (New England Biolabs) was incubated for 30 min at 37 °C. The NPP reaction mixture (10 μL) containing 50 mM Tris·HCl (pH 8.0), 10 mM $MgCl_2$, 100 mM NaCl, and 0.001 U NPP (Sigma) was incubated for 20 min at 37 °C. The P1 reaction mixture (10 μL) containing 50 mM sodium acetate (pH 5.2), 1 mM $ZnCl_2$, and 0.5 U nuclease P1 (Sigma) was incubated for 20 min at 50 °C. For double digestions with NPP and CIP the samples were initially digested with NPP as described above, then the mixtures were adjusted to CIP buffer and subsequently treated with CIP as above. For double digestions with P1 and CIP the samples were initially digested with P1 as described above, then the mixtures were adjusted to CIP buffer and subsequently treated with CIP as above. All digestion reactions were quenched by adding 2 μL of 50 mM EDTA. Aliquots (6 μL) of the untreated and digested DNAs were applied to a PEI-cellulose TLC plate (Merck); each sample was overlaid with cold GTP, GDP, and GMP markers. The mobile phase for ascending TLC was 1 M LiCl. The radiolabeled species were visualized by autoradiography; the cold markers were localized by UV illumination.

Identification of the Site of Covalent Guanylylation. A reaction mixture (10 μL) containing 50 mM Tris·HCl (pH 8.0), 2 mM $MnCl_2$, 5 μM RtcB, and 10 μM unlabeled GTP was incubated at 37 °C for 1 min, then quenched with 1 μL of 50 mM EDTA and diluted to 100 μL with 50 mM ammonium bicarbonate (pH 8.0). An aliquot (25 μL) was adjusted to 10 mM DTT and incubated at 57 °C for 1 h, after which the mixture was supplemented with iodoacetamide (20 mM concentration) and incubated in the dark for 45 min at room temperature. The alkylated protein was recovered by methanol:chloroform extraction, resuspended in 50 μL ammonium bicarbonate (pH 8.0), and then treated with 5 μg of trypsin for 16 h at 25 °C. The proteolysis was quenched by adding 50 μL of 0.1% trifluoroacetic acid in 40% (vol/vol) acetonitrile.

The tryptic peptides were resolved by applying the digest to a reverse-phase C18 (YMC, 15 μm, 300 A) column (75-μm internal diameter) and eluting the bound material with a linear gradient of 0–70% acetonitrile in 0.5% acetic acid over 60 min at a flow rate of 160 nL/min). The eluate was sprayed directly into a mass spectrometer (LTQ-Orbitrap-XL-ETD; Thermo Fisher Sci-

entific) for analysis (19). The repetitive analytical cycle comprised two stages. First, a high-resolution mass scan (res = 60,000) of intact ions was analyzed by Orbitrap. Next, fragmentation of 10 of the most intense peaks in the previous scan was carried out by collision-induced dissociation (CID). All CID fragments were analyzed with a linear ion trap. The *.raw mass spectral files were analyzed by MaxQuant (ver. 1.1.1.36) for the presence of a guanylate adduct (26). Spectra of the peptide containing a putative GMP modification were verified manually.

ACKNOWLEDGMENTS. This research was supported by National Institutes of Health Grants GM46330 (to S.S.) and RR00862 (to B.T.C.). S.S. is an American Cancer Society Research Professor.

1. Shuman S, Lima CD (2004) The polynucleotide ligase and RNA capping enzyme superfamily of covalent nucleotidyltransferases. *Curr Opin Struct Biol* 14:757–764.
2. Schwer B, Sawaya R, Ho CK, Shuman S (2004) Portability and fidelity of RNA-repair systems. *Proc Natl Acad Sci USA* 101:2788–2793.
3. Nandakumar J, Schwer B, Schaffrath R, Shuman S (2008) RNA repair: An antidote to cytotoxic eukaryal RNA damage. *Mol Cell* 31:278–286.
4. Martins A, Shuman S (2005) An end-healing enzyme from *Clostridium thermocellum* with 5′ kinase, 2′,3′ phosphatase, and adenylyltransferase activities. *RNA* 11:1271–1280.
5. Chan CM, Zhou C, Huang RH (2009) Reconstituting bacterial RNA repair and modification in vitro. *Science* 326:247.
6. Greer CL, Peebles CL, Gegenheimer P, Abelson J (1983) Mechanism of action of a yeast RNA ligase in tRNA splicing. *Cell* 32:537–546.
7. Konarska M, Filipowicz W, Gross HJ (1982) RNA ligation via 2′-phosphomonoester, 3′5′-phosphodiester linkage: Requirement of 2′,3′-cyclic phosphate termini and involvement of a 5′-hydroxyl polynucleotide kinase. *Proc Natl Acad Sci USA* 79: 1474–1478.
8. Gonzalez TN, Sidrauski C, Dörfler S, Walter P (1999) Mechanism of non-spliceosomal mRNA splicing in the unfolded protein response pathway. *EMBO J* 18:3119–3132.
9. Amitsur M, Levitz R, Kaufmann G (1987) Bacteriophage T4 anticodon nuclease, polynucleotide kinase and RNA ligase reprocess the host lysine tRNA. *EMBO J* 6: 2499–2503.
10. Filipowicz W, Shatkin AJ (1983) Origin of splice junction phosphate in tRNAs processed by HeLa cell extract. *Cell* 32:547–557.
11. Laski FA, Fire AZ, RajBhandary UL, Sharp PA (1983) Characterization of tRNA precursor splicing in mammalian extracts. *J Biol Chem* 258:11974–11980.
12. Filipowicz W, Konarska M, Gross HJ, Shatkin AJ (1983) RNA 3′-terminal phosphate cyclase activity and RNA ligation in HeLa cell extract. *Nucleic Acids Res* 11:1405–1418.
13. Tanaka N, Shuman S (2011) RtcB is the RNA ligase component of an *Escherichia coli* RNA repair operon. *J Biol Chem* 286:7727–7731.
14. Popow J, et al. (2011) HSPC117 is the essential subunit of a human tRNA splicing ligase complex. *Science* 331:760–764.
15. Englert M, Sheppard K, Aslanian A, Yates JR, 3rd, Söll D (2011) Archaeal 3′-phosphate RNA splicing ligase characterization identifies the missing component in tRNA maturation. *Proc Natl Acad Sci USA* 108:1290–1295.
16. Tanaka N, Meineke B, Shuman S (2011) RtcB, a novel RNA ligase, can catalyze tRNA splicing and *HAC1* mRNA splicing *in vivo*. *J Biol Chem* 286:30253–30257.
17. Okada C, Maegawa Y, Yao M, Tanaka I (2006) Crystal structure of an RtcB homolog protein (PH1602-extein protein) from *Pyrococcus horikoshii* reveals a novel fold. *Proteins* 63:1119–1122.
18. Tanaka N, Chakravarty AK, Maughan B, Shuman S (2011) Novel mechanism of RNA repair by RtcB via sequential 2′,3′-cyclic phosphodiesterase and 3′-Phosphate/5′-hydroxyl ligation reactions. *J Biol Chem* 286:43134–43143.
19. Olsen JV, et al. (2009) A dual pressure linear ion trap Orbitrap instrument with very high sequencing speed. *Mol Cell Proteomics* 8:2759–2769.
20. Samai P, Shuman S (2011) Functional dissection of the DNA interface of the nucleotidyltransferase domain of *chlorella* virus DNA ligase. *J Biol Chem* 286:13314–13326.
21. Nandakumar J, Shuman S (2004) How an RNA ligase discriminates RNA versus DNA damage. *Mol Cell* 16:211–221.
22. Jackman JE, Phizicky EM (2006) $tRNA^{His}$ guanylyltransferase catalyzes a 3′-5′ polymerization reaction that is distinct from G_{-1} addition. *Proc Natl Acad Sci USA* 103: 8640–8645.
23. Tanaka N, Smith P, Shuman S (2010) Structure of the RNA 3′-phosphate cyclase-adenylate intermediate illuminates nucleotide specificity and covalent nucleotidyl transfer. *Structure* 18:449–457.
24. Filipowicz W, Strugala K, Konarska M, Shatkin AJ (1985) Cyclization of RNA 3′-terminal phosphate by cyclase from HeLa cells proceeds via formation of N(3′)pp(5′)A activated intermediate. *Proc Natl Acad Sci USA* 82:1316–1320.
25. Chakravarty AK, Shuman S (2011) RNA 3′-phosphate cyclase (RtcA) catalyzes ligase-like adenylylation of DNA and RNA 5′-monophosphate ends. *J Biol Chem* 286: 4117–4122.
26. Cox J, Mann M (2008) MaxQuant enables high peptide identification rates, individualized p.p.b.-range mass accuracies and proteome-wide protein quantification. *Nat Biotechnol* 26:1367–1372.